Structural Safety 36–37 (2012) 23–31

Contents lists available at SciVerse ScienceDirect

Structural Safety

journal homepage: www.elsevier.com/locate/strusafe

A three-stage resilience analysis framework for urban infrastructure systems

Min Ouyang [a,b,*], Leonardo Dueñas-Osorio [a], Xing Min [a]

[a] Department of Civil and Environmental Engineering, Rice University, 6100 Main Street, MS-318, TX 77005, United States
[b] Department of Control Science and Engineering, Huazhong University of Science and Technology, 1037 Luoyu Road, Wuhan 430074, China

ARTICLE INFO

Article history:
Received 23 February 2011
Received in revised form 7 November 2011
Accepted 9 December 2011
Available online 13 March 2012

Keywords:
Infrastructure systems
Multiple hazards
Expected annual resilience
Power systems

ABSTRACT

This paper proposes a new multi-stage framework to analyze infrastructure resilience. For each stage, a series of resilience-based improvement strategies are highlighted and appropriate correlates of resilience identified, to then be combined for establishing an expected annual resilience metric adequate for both single hazards and concurrent multiple hazard types. Taking the power transmission grid in Harris County, Texas, USA, as a case study, this paper compares an original power grid model with several hypothetical resilience-improved models to quantify their effectiveness at different stages of their response evolution to random hazards and hurricane hazards. Results show that the expected annual resilience is mainly compromised by random hazards due to their higher frequency of occurrence relative to hurricane hazards. In addition, under limited resources, recovery sequences play a crucial role in resilience improvement, while under sufficient availability of resources, deploying redundancy, hardening critical components and ensuring rapid recovery are all effective responses regardless of their ordering. The expected annual resilience of the power grid with all three stage improvements increases 0.034% compared to the original grid. Although the improvement is small in absolute magnitude due to the high reliability of real power grids, it can still save millions of dollars per year as assessed by energy experts. This framework can provide insights to design, maintain, and retrofit resilient infrastructure systems in practice.

1. Introduction

Modern societies are increasingly dependent on infrastructure systems to provide essential services that support economic prosperity and quality of life [1]. Most of these infrastructure systems are networked in nature and the failures of some system components can result in the disruptions of other components via cascading failures. To understand infrastructure system performance under random failures, manmade attacks and natural hazards, some researchers have focused on the modeling and simulation of cascading failures of infrastructure systems [2–5], while others have addressed and modeled the systems' restoration processes [6–9]. The full consideration of both aspects is pertinent to infrastructure system resilience, which facilitates communication to the public and enables an informed adoption of infrastructure protection policies. In fact, the president of the United States [10] proclaimed that "Our goal is to ensure a more *resilient* Nation—one in which individuals, communities, and our economy can adapt to changing conditions as well as withstand and rapidly recover from disruptions due to emergencies." To realize this goal, designing and striving for resilient infrastructure systems is essential.

Regarding the definitions of resilience, they vary by discipline and application. The ecologist Holling defined resilience at the system level as "a measure of the persistence of systems and of their abilities to absorb change and disturbance and still maintain the same relationships between populations or state variables" [11]. The US Department of Homeland Security conceptualized resilience as "the capacity of an asset, system, or network to maintain its function during or to recover from a terrorist attack or other incident" [12]. The Multidisciplinary Center for Earthquake Engineering Research (MCEER) de fined resilience as "the ability of the system to reduce the chances of shock, to absorb a shock if it occurs and to recover quickly after a shock (re-establish normal performance)" [6]. In addition, from a systems and information engineering perspective, Haimes [13] defined resilience as the ability of the system to withstand a major disruption within acceptable degradation parameters and to recover within an acceptable time and composite costs and risks, while Aven [14], with a risk management angle, defined resilience as the uncertainty about and severity of the consequences of the activity given the occurrence of any types of events. More definitions are summarized in recent publications [7,15]. As a synthesis of the available literature, this paper defines resilience as the joint ability of infrastructure systems to *resist* (prevent and withstand) any possible hazards, *absorb* the initial damage, and *recover* to normal operation.

To quantify or assess resilience, many researchers have proposed different methods or frameworks. Bruneau et al. introduced

* Corresponding author at: Department of Civil and Environmental Engineering, Rice University, 6100 Main Street, MS-318, TX 77005, United States.
E-mail addresses: min.ouyang@rice.edu (M. Ouyang), leonardo.duenas-osorio@rice.edu (L. Dueñas-Osorio), xing.min@rice.edu (X. Min).

0167-4730/$ - see front matter © 2011 Elsevier Ltd. All rights reserved.
doi:10.1016/j.strusafe.2011.12.004

a general framework to define seismic resilience of communities or any type of physical and organizational systems and identified some quantitative measures of resilience [6]. In this framework, resilience includes four properties: robustness, redundancy, resourcefulness, and rapidity, while resilience is quantified with four interrelated dimensions: technical, organizational, social and economic. Based on this framework, various studies have been carried out to assess the resilience of practical engineered systems, and quantify the resilience from different perspectives to support improvement decisions. For instance, Chang and Shinozuka quantified resilience as the probability that the system would meet both robustness and rapidity standards in a specific event, with the application to a water delivery system to compare two seismic retrofit strategies [16]. Bruneau and Reinhorn related fragility functions and seismic resilience in a single integrated approach for acute care facilities, and the resilience level was measured by the percentage of healthy population and the number of patients/day that can receive service [17]. Combining the Bruneau's seismic resilience framework, input–output models and structural fragilities, Reed et al. introduced a simple methodology to quantify engineering resilience for subsystems of a multi-system infrastructure system under extreme natural hazards [8]. Then, Cimellaro et al. provided a resilience metric as the area beneath the performance curve over a given period defined as the control time [9,18], while Zobel presented different adjusted resilience metrics based on robustness and rapidity, with the consideration of the preferences and priorities of a given decision maker [19]. Also, Vugrin et al. [7] reasoned that the quantification of system resilience should take into account the recovery cost as an additional consideration relative to the prevailing studies on infrastructure resilience.

Most previous research is usually aimed at specific disruptive events or single hazards, such as earthquakes, hurricanes or others, while rarely considering system resistive, absorptive and restorative capacities together, and not accounting for the occurrence of joint hazards. Hence, this paper introduces a three-stage resilience analysis *framework* that addresses current modeling gaps, where a resilience parameter measures the joint ability of infrastructure systems to *resist* (prevent and withstand) any possible hazards, *absorb* the initial damage, and *recover* to normal operation levels. The occurrence rates of different hazard types are also integrated into an expected annual resilience metric. The rest of this paper is organized as follows: Section 2 introduces the proposed three-stage resilience analysis framework. A series of emerging strategies from the literature to improve infrastructure resilience are synthesized, and an expected annual resilience metric adequate for both single hazards and multiple hazard types is also proposed. Taking the power transmission grid in Harris County, Texas as an example, Section 3 compares a conventional power grid model with several hypothetical resilience-improved models in terms of the effectiveness of improvement strategies at different resilience stages. Finally, Section 4 provides conclusions and includes directions for future research.

2. Three-stage resilience analysis framework

2.1. Three-stage resilience concept

To propose a framework for resilience analysis, this section introduces first a typical infrastructure system performance response process following the occurrence of a hazard, as shown in Fig. 1. The performance level can be measured by different metrics, such as the amount of flow or services delivered, the availability of critical facilities, the number of people served, and the level of economic activity, which correspond to different dimensions of resilience [6]. This paper mainly focuses on the technical dimension

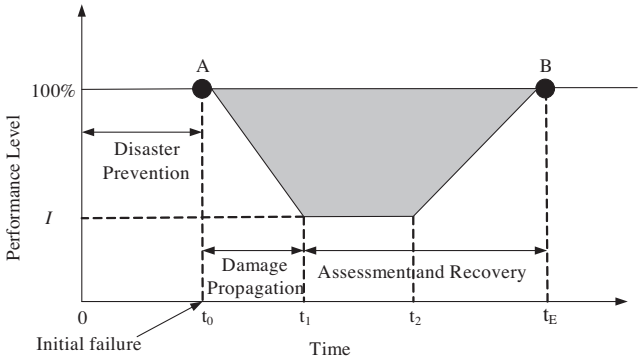

Fig. 1. Typical performance response curve of an infrastructure system following a disruptive event.

of resilience, and the performance level is measured by the number of normally operating components within an infrastructure system.

Note that the performance response process in Fig. 1 can be divided into three different stages. The first stage ($0 \leqslant t \leqslant t_0$) is the disaster prevention stage from normal operation to the onset of initial failure. It mainly reflects the resistant capacity of the system as its ability to prevent any possible hazards and reduce the initial damage level if a hazard occurs. Two indexes "hazard frequency" and "initial damage level" together describe the resistant capacity concept, and are taken as the resilience correlates in the first stage of the proposed framework. The second stage ($t_0 < t \leqslant t_1$) is the damage propagation process after initial failures. It mainly reflects the absorptive capacity of the system as the degree to which it absorbs the impacts of initial damage and minimizes the consequences, such as cascading failures. The maximum impact level ($1 - I$ in Fig. 1) is used to measure the absorptive capacity and regarded as the resilience correlate in the second stage. The third stage ($t_1 < t \leqslant t_E$) is the recovery process during which system damage information is collected for assessment, and resources are allocated to restore performance. The new steady-state performance level may be better or worse than the original performance state. This stage mainly reflects the restorative capacity, which is the ability of the system to be repaired quickly and effectively. Recovery time and recovery cost together represent the restoration capacity and help characterizing resilience in the third stage.

The three stages constitute together a typical infrastructure response cycle to disruptions. The first stage mainly focuses on local level impacts, translating hazards into component-level failures. The second stage emphasizes system-level effects, translating initial local component failures into system-level consequences. The third stage characterizes the restoration response, translating external efforts into system recuperation. To enhance system resilience, improvement strategies can be grouped at different stages. Table 1 lists some sample strategies for enhanced infrastructure resilience in practice.

In the case study of this paper, the power transmission grid in Harris County, Texas USA is used as an example to illustrate capacity enhancement approaches. As Harris County is located near the Gulf Coast which experiences on average a hurricane once every 7 years [29], two main hazard types are considered: random hazards and hurricane hazards. Random hazards are a collective name for different hazard types, such as human errors, tree-induced failures, and animal related events, which only cause a small portion of the infrastructure system components to initially fail, and that in aggregate have a high degree of uncertainty.

To establish a resilience-improved power grid model in this work, different feasible strategies are used at different stages. In the first stage, the new power system has a reduced frequency of

Table 1
Sample strategies to improve infrastructure system resilience per response process stage.

Stage	Stage resilience correlates	Resilience improvement strategies [sample applications]
First stage (resistant capacity)	Hazard frequency, initial damage level	• Use risk management methods to identify and harden key components [20] • Learn and improve from previous accidents using accident models, such as the Systems-Theoretic Accident Model and Processes (STAMP) approach [21] • Sense, monitor, and update system states in real time along with state visualizations based on emerging infrastructure modeling techniques, such as Bayesian networks [22]. • Improve decision support platforms, staff training, and organizational culture to enhance situational awareness [23]
Second stage (absorptive capacity)	Maximum impact level ($1-I$)	• Adjust infrastructure system topology [24] • Design for system redundancy [25] • Add self-healing and self-adapting infrastructure system response mechanisms [26]
Third stage (restorative capacity)	Recovery time, recovery cost	• Establish efficient communication channels and coordination for rapid recovery response [27] • Improve decision support platforms to quickly and accurately identify feasible recovery strategies [28]

random hazards by preventing the occurrence of possible accidents according to lessons learned from previous accidents, by adopting real-time monitoring for early warning of the potential accidents, and by hardening some critical components identified by risk management methods so that they have improved fragility to resist damage. In the second stage, the new power system is deployed with energy storage and emergency generators in some power substations so that the local customers can still get electricity after the outages of the corresponding load substations. In the third stage, the new system is provided with faster recovery responses and optimized or sub-optimized recovery sequences. A numerical example with the impact of these three-stage strategies on power grid resilience is presented in Section 3.

2.2. Infrastructure resilience metric

As the hazard frequency is one of the stage resilience correlates, this paper introduces a novel time-dependent expected annual resilience (AR) metric as the mean ratio of the area between the real performance curve and the time axis to the area between the target performance curve and the time axis during a year. This resilience metric differs from existing ones in that it can incorporate multiple inter-related hazards as follows:

$$AR = E\left[\frac{\int_0^T P(t)dt}{\int_0^T TP(t)dt}\right] = E\left[\frac{\int_0^T TP(t)dt - \sum_{n=1}^{N(T)} AIA_n(t_n)}{\int_0^T TP(t)dt}\right] \quad (1)$$

where $E[\bullet]$ is the expected value; T is a time interval for a year (T = 1 year = 365 days); $P(t)$ the actual performance curve, which is a stochastic process; $TP(t)$ the target performance curve, which can be a constant line or a stochastic process; n the event occurrence number, including event co-occurrences of different hazard types; $N(T)$ the total number of event occurrences during T; t_n the occurrence time of the nth event which is a random variable; and $AIA_n(t_n)$ is the area between the real performance curve and the targeted performance curve, called impact area, for the nth event occurrence at time t_n. Details for computing $AIA_n(t_n)$ for different hazard cases (single and multiple joint hazard types) are provided in the subsections below. For practical applications, if $TP(t)$ is a constant line (as assumed in the case study), i.e. $TP(t) = TP$, and the infrastructure system is restored to its original condition after each event occurrence, then Eq. (1) reduces to the following:

$$AR = \frac{TP \times T - E\left[\sum_{n=1}^{N(T)} AIA_n(t_n)\right]}{TP \times T} = \frac{TP - E\left[\frac{1}{T}\sum_{n=1}^{N(T)} AIA_n(t_n)\right]}{TP} \quad (2)$$

where the impact area $AIA_n(t_n)$ is a random variable with high uncertainties that is a function of the hazard types for the nth event, and the remaining four stage resilience correlates: the initial damage level from the hazards, the maximum impact level from the hazards, the restoration time, and the restoration cost (efforts). Hence, the resilience Eqs. (1) and (2) are adequate for both single hazards and multiple hazard types which include their simultaneous occurrence (i.e., the nth event may be the co-occurrence event of different hazard types), capture the frequency variations that may be present in $N(T)$, and include fluctuations in $AIA_n(t_n)$ as it may also vary for the nth event due to the resource allocations or the preventive measures taken for other hazard events. This conceptual flexibility in Eq. (2) prevents its representation by a more specific expression. Hence, to add specificity for illustrative purposes, this paper assumes that the occurrence of each hazard type $h = 1,2,\ldots,$ H is modeled by a Poisson process which is not unrealistic for hurricanes or random hazards, with respective occurrence rates of v^h per year. Then, the expected annual resilience of Eq. (2) can be specialized for both single hazards and multiple hazard types.

2.2.1. Resilience under single hazard type

Under the assumption of Poisson processes governing the occurrence of a hazard type, and considering each hazard independent, the expectation term in Eq. (2) for a single hazard h is simplified as follows:

$$E\left[\frac{1}{T}\sum_{n=1}^{N(T)} AIA_n(t_n)\right] = \frac{1}{T}\sum_{N=0}^{\infty} N \times E\left[AIA^h\right]\frac{(v^hT)^N e^{-v^hT}}{N!} = v^h E\left[AIA^h\right] \quad (3)$$

where $E[AIA^h]$ is the expected impact area under hazard type h accounting for all any possible hazard intensities. More specifically, denote the hazard intensity by q^h, which can be a variable representing the maximum or average hazard intensity level at different infrastructure component sites, or a vector of variables describing the hazard intensity at each infrastructure component site, and also define $\varphi^h(q^h)$ as the probability density function for q^h or the probability mass function $\Phi^h(q^h)$ if q^h is a discrete variable. Then the expectation term in the right hand side of Eq. (3) can be expanded as follows:

$$\begin{aligned} E\left[AIA^h\right] &= E\left[E\left[AIA^h(q^h)\right]\right] \\ &= \int_{q^h} E\left[AIA^h(q^h)\right]\varphi^h(q^h)dq^h \text{ or } \sum_{q^h} E\left[AIA^h(q^h)\right]\Phi^h(q^h) \end{aligned} \quad (4)$$

where $E[AIA^h(q^h)]$ is the expected impact area under a given hazard intensity q^h. If the distributions of initial damage level, the maximum impact level, the restoration time and the restoration cost affecting $AIA^h(q^h)$ are known, Eq. (4) can be expanded accordingly. Hence, Eq. (4) provides expressions for expected annual resilience assessment under a single hazard type, while enabling integration of all five identified resilience correlates if appropriately expanded.

2.2.2. Resilience under multiple hazard types

Consider the general case with H types of hazards, each modeled by a Poisson process with occurrence rate v^h, $h = 1,2,\ldots,H$, and the mean duration u^h, $h = 1,2,\ldots,H$. Then, the co-occurrences of multiple hazards can be also modeled by a Poisson process [30,31], which simplifies the expectation term in Eq. (2) into the following expressions:

$$E\left[\frac{1}{T}\sum_{n=1}^{N(T)} AIA_n(t_n)\right] = \sum_{h=1}^{H}\lambda^h E[AIA^h] + \sum_{h=1}^{H-1}\sum_{i=h+1}^{H}\lambda^{hi}E[AIA^{hi}] + \sum_{h=1}^{H-2}\sum_{i=h+1}^{H-1}\sum_{j=i+1}^{H}\lambda^{hij}E[AIA^{hij}] + \ldots. \quad (5)$$

where

$$\lambda^h = v^h - \sum_{\substack{i=1\\ i\neq h}}^{H} v^{hi} + \frac{1}{2}\sum_{\substack{i=1\\ i\neq h}}^{H}\sum_{\substack{j=1\\ j\neq h,i}}^{H} v^{hij} - \frac{1}{6}\sum_{\substack{i=1\\ i\neq h}}^{H}\sum_{\substack{j=1\\ j\neq h,i}}^{H}\sum_{\substack{k=1\\ k\neq h,i,j}}^{H} v^{hijk} + \ldots \quad (6)$$

$$\lambda^{hi} = v^{hi} - \sum_{\substack{j=1\\ j\neq h,i}}^{H} v^{hij} + \frac{1}{2}\sum_{\substack{j=1\\ j\neq h,i}}^{H}\sum_{\substack{k=1\\ k\neq h,i,j}}^{H} v^{hijk} - \ldots \quad (7)$$

$$\lambda^{hij} = v^{hij} - \sum_{\substack{k=1\\ k\neq h,i,j}}^{H} v^{hijk} + \ldots \quad (8)$$

$$v^{hi} = v^h v^i (u^h + u^i) \quad (9)$$

$$v^{hij} = v^h v^i v^j (u^h u^i + u^i u^j + u^h u^j) \quad (10)$$

$$v^{hijk} = v^h v^i v^j v^k (u^h u^i u^j + u^h u^i u^k + u^i u^j u^k + u^h u^j u^k) \quad (11)$$

and v^h, v^{hi}, v^{hij}, v^{hijk} are the mean occurrence rate of hazard type h, mean co-occurrence rate of two hazard types (h, i), three hazard types (h, i, j), and four hazard types (h, i, j, k), respectively; λ^h, λ^{hi}, λ^{hij} are the mean occurrence rates of individual hazard types h without accounting for the co-occurrence of hazard type h with other hazard types, mean co-occurrence rate of two hazard types (h, i) without accounting for the co-occurrence of hazard type hi with other hazard types, and mean co-occurrence rate of three hazard types (h, i, j) without accounting for the co-occurrence of hazard type hij with other hazard types, respectively; and $E[AIA^h]$, $E[AIA^{hi}]$, $E[AIA^{hij}]$ are the expected impact areas under one hazard type h, two co-occurrence hazard types (h, i) and three co-occurrence hazard types (h, i, j), respectively, from possible hazard intensities. Note that calculating the co-occurrence rate of multiple hazards requires the mean duration u^h of each hazard type, but the value of u^h is affected by the restoration cost. Hence, it is possible to assign u^h a value range in advance given the restoration cost, so that a value range of the expected annual resilience can be computed to bound the real expected annual resilience. However, if the co-occurrence rates of multiple hazards are neglected, it is not necessary to consider u^h, and the expected annual resilience under multiple hazard types is provided as follows:

$$AR = \frac{TP - \sum_{h=1}^{H} v^h \int_{q^h} E[AIA^h(q^h)]\varphi^h(q^h)dq^h}{TP} \quad \text{or} \quad \frac{TP - \sum_{h=1}^{H} v^h \sum_{q^h} E[AIA^h(q^h)]\Phi^h(q^h)}{TP} \quad (12)$$

The case study of this paper will consider this special case in which each hazard type is modeled by a Poisson process while the co-occurrences of different hazard types are ignored.

3. Case study for infrastructure resilience assessment

This section takes the power transmission grid in Harris County, Texas USA as an example to simulate its resilience and discuss its resilience-based improvements under multiple hazard types. The original power system data is obtained from Platts [32]. Its geographical representation is shown in Fig. 2. There are 417 nodes, 23 of them are generators nodes and other nodes are all assumed as load points or substations. These nodes are linked by 551 transmission and sub-transmission lines with a total length of 2144.5 km.

3.1. Hazard types

As Harris County is located near the Gulf Coast which experiences on average a hurricane of category 1 or higher about once every 7 years, this paper mainly considers two hazard types for illustrative purposes: random hazards (which are mostly shared across power systems regardless of location) and hurricane hazards.

3.1.1. Random hazards

Random hazards are a collective name for hazards, such as equipment failures, vegetation (trees), animals, and human errors, which only cause a small portion of the infrastructure system components to initially fail and are highly uncertain so that their damage impacts are justifiable modeled as random failures. As the collection of random hazards have different hazard sources, it is difficult to find a realistic metric to quantify the hazard intensity. Hence, assuming that the cumulative effect of random hazards can be quantified by a single metric, this paper introduces an impact size metric for random hazard intensity, with discrete values $1,2,3,\ldots$, which determines the number of initial randomly failed components. Also, some recent investigations on power system blackouts have shown that the blackout time intervals for power systems approximately satisfies the exponential distribution [33]. Hence, the random hazards can be modeled by a Poisson process. According to historical data [34,35], for the power transmission system in Harris County, the yearly occurrence rate of random hazards is $v^1 = 19$/year, where the superscript $h = 1$ indicates random hazards, while the distribution of the hazard intensity can be modeled by a power law distribution: $\Phi^1(q^1 = x) = 0.905x^{-3.7}$, $1 \leqslant x \leqslant 8$, where x is the hazard intensity level. The range limitation of x describes the empirical small portion of initial failed components under random hazards [35].

3.1.2. Hurricane hazards

For the hurricane hazards, their occurrences can be modeled by a Poisson process as well [30,31]. Also, according to historical data from 1900 to 1999 [35], the return periods of hurricanes with

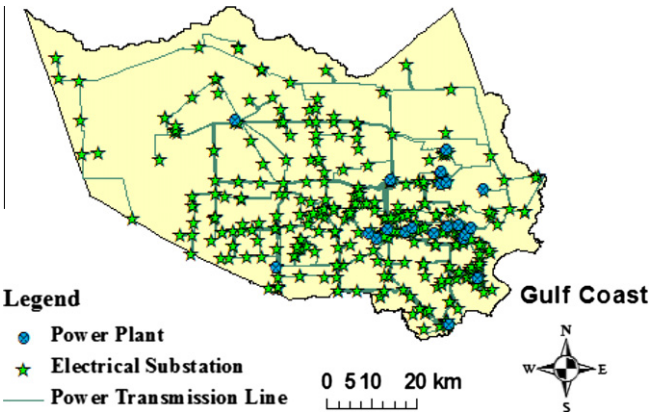

Fig. 2. A geographical representation of the power transmission grid in Harris County, Texas.

Table 2
Hurricane categories and their return period in Harris County, Texas.

Category q^2	1	2	3	4	5
Wind speed (m/s)	33–42	43–49	50–58	59–69	>70
Return period in Harris County (years)	7	15	25	53	140
Category probability of a future hurricane $\Phi^2(q^2)$	0.5333	0.1867	0.1479	0.0821	0.05

different categories in Harris County are listed in Table 2. The empirical probability of a hurricane belonging to each category is also computed and shown in the same table. Based on these data, the occurrence rate of hurricane hazards with category 1 or higher per year is $\nu^2 = 1/7/$ year, where the superscript $h = 2$ indicates hurricane hazards. If wind speeds are used as the hurricane intensity metric q^2, and as the wind speeds at different infrastructure component sites vary largely, the parameter q^2 should be a vector of variables representing the wind speed at each infrastructure component site of interest, and in theory the $\varphi^2(q^2)$ function should be a joint probability density function. However, it is difficult to get $\varphi^2(q^2)$ in practice, so this paper defines q^2 as the hurricane category, i.e. $q^2 \in \{1,2,3,4,5\}$, and uses the HAZUS-MH3 software to generate 50 scenario-based wind fields for each q^2 to provide estimates of wind gusts at each component site [36]. The discrete probability distribution $\Phi^2(q^2)$ is shown in Table 2. To capture the hurricane hazard geographical variability for a given a hurricane intensity (category) during infrastructure performance assessments, a pre-generated hurricane scenario is randomly selected among those scenarios from HAZUS-MH3. The wind gust speeds at different sites for different scenarios can then be used in the required simulations to estimate system resilience under hurricane hazards.

3.2. Original and hypothetical resilience-improved power grids

The expected annual resilience metric is computed for both the original and improved power grids, where the key is to obtain the expected impact area $E[AIA^h(q^h)]$ for each hazard $h = \{1,2\}$ given q^h. Hence, this subsection first presents the procedures to simulate the real performance response curve for the power system given q^h, to then calculate the $AIA^h(q^h)$ function. Details of the original and hypothetically improved models are also introduced in this subsection.

3.2.1. Procedures to simulate the real performance response curve

To model the power system response under a disruptive event, and due to unavailability of power injection and line susceptance data, this paper uses a complex network betweenness model [3]. If a substation betweenness exceeds its maximum capacity defined as the product of its initial betweenness and a tolerance parameter (tp), this substation fails operationally. This model has been validated to approximate the necessary yet not sufficient conditions for operation [37]. In addition, to focus on the effectiveness of different resilience improvement strategies, this paper does not consider a recovery model to describe the *dynamic* resource mobilization process and the effects of different recovery costs on recovery speeds [25], but simply models the recovery cost by the amount of recovery resources, r, as a generic single value of available resource units, and each damaged component is assumed to only require one unit of resources for recovery. Here, one unit of resources means a work team including repair crews, vehicles, equipments and some replacement components. Fig. 3 gives the flow chart to simulate the performance response of power systems given q^h. As the recovery process in days or weeks scales is usually much longer than the damage propagation process in seconds or minutes scales, i.e. $t_E - t_1 \gg t_1 - t_0$ in Fig. 1, the damage propagation process is assumed instantaneous as an approximation in the simulation. A description of Fig. 3 is as follows:

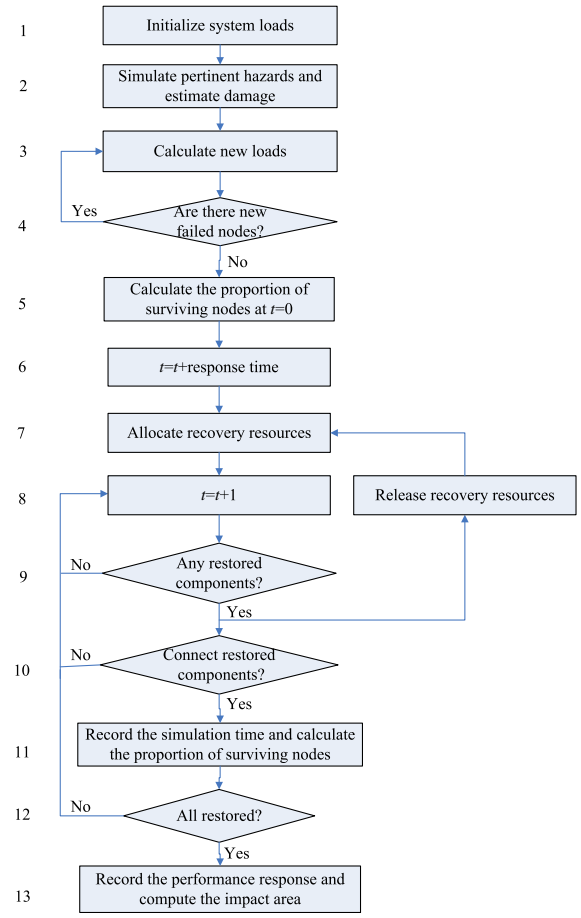

Fig. 3. Flow chart to simulate the performance response of infrastructure systems under single hazards.

1. Calculate the initial node loads (betweenness) and node capacities [3].
2. Simulate random hazards or hurricane hazards under given q^h, $h = 1,2$. For random hazards, randomly select q^1 components to fail and assign each failed component a repair time, which is the sum of a variable ε satisfying the uniform distribution [0,3 h] and a variable η satisfying the exponential distribution with mean value 5 h, as set by Anghel et al. [38]. Here, ε describes the traffic time for dispatching resources and η is the time to restore the failed components, both in units of hours.
   For hurricane hazards, randomly select a wind field from the pre-generated hurricane scenarios per hurricane category q^2, and obtain specific wind gusts at the site of each power substations and transmission lines. Then based on the component fragility model proposed by Winkler [37], first generate four damage probabilities $p_i^L > p_i^M > p_i^S > p_i^D$, corresponding to four damage levels of the substations: low, moderate, severe and complete. Compare these probabilities

with a uniformly distributed random variable $\chi \in [0,1]$ to determine the damage level realizations per substation. Then, for each failed substation, assign a repair time in days (d), which satisfies a normal distribution with mean value (standard deviation) of 1d (0.5d), 3d (1.5d), 7d (3.5d) and 30d (15d) for low, moderate, severe and complete damage levels, respectively, as suggested in HAZUS-MH3 [36]. Also, for each transmission line, calculate its failure probability according to Winkler's fragility model [37] and then compare this probability with a uniformly distributed random variable $\chi \in [0,1]$ to determine its status. For each failed line, assume its repair time satisfies a normal distribution with mean value 1d and standard deviation 0.5d.

3. Remove the failed components from the network and recalculate the node loads.
4. Find the failed nodes violating their capacity limits. For each failed node assign it a repair time, which is the sum of ε and η, and then go to step 3; otherwise, go to step 5.
5. Calculate the proportion of surviving nodes, corresponding to the impact level I. Mark the time $t = 0$, as the time when the performance curve sharply changes from 1 to I.
6. Move to time $t = t$ + response time (for failure detections and restoration decisions).
7. Allocate r resources to the unrestored components according to the recovery sequences (determined in Section 3.2.2).
8. Move to time $t = t + 1$ as the next restoration time.
9. Find the restored components with the repair time reaching their preset values. If restored components exist, release the resources and reallocate them to unrestored components, and then go to step 10; otherwise, go to step 8.
10. Reconnect restored components, and calculate new network loads. If they lead to new overloaded nodes, cancel the reconnections and go to step 8; otherwise, go to step 11.
11. Get the new network topology of the stable system, and record the time and the proportion of surviving nodes.
12. Assess whether all components have been restored. If so, go to step 13; otherwise, go to step 8;
13. Record the real performance response duration for restoration, and calculate the impact area $AIA^h(q^h)$.

Repeat the above steps 500 times so that the expected impact area $E[AIA^h(q^h)]$ converges given q^h. With the value of $E[AIA^h(q^h)]$ under different q^h and taking the distributions of q^h into consideration, it is possible to calculate the expected annual resilience under both single hazards and multiple hazard types according to Eq. (12). Also, in the above simulation process, different resilience improvement strategies from the first to the third stage (Table 1) can be modeled in three groups of algorithm steps: 2, 3–5, and 6–12, respectively. Details regarding these strategies for resilience enhancement are introduced next.

3.2.2. Differences between original and hypothetical resilience-improved grids

Preventive strategies or improvement resources may simultaneously affect the resilience under different hazard types. However, this paper does not focus on maximizing the interacting mechanisms between the improvement resources (or strategies) for a given hazard and their impacts on different hazard types. Instead, the objective is to use typical and emerging strategies to increase infrastructure resilience and illustrate their outcomes (or the effectiveness from specific resource allocations) at different stages associated with the simulation steps in the flow chart of Fig. 3. Specifically, in the first resistant resilience stage and relative to the original power grid, a resilience-improved system is assumed to have a reduced frequency of random hazards from 19 to 17, which changes the value of occurrence rate v^1 in the resilience Eq. (12). Under hurricane hazards, the four types of substation fragility curves that describe the probabilities of low, moderate, severe and complete damage, are improved via their logarithmic mean value by 1%, 0.5%, 0.2%, 0.1%, respectively, for 10% of the most critical substations. These substations are identified in terms of their maximum topological degrees. These improvements are reflected in step 2 in the flow chart.

In the second absorptive resilience stage, relative to the original power grid, a resilience-improved system is assumed to possess energy storage and emergency generator capabilities (Table 1) in 10% of the critical substations. These substations are identified according to their maximum topological degrees, and can still distribute power for a period of time (up to 24 h as the minimum capacity value suggested by researchers [39]) after their failures. These improvements are implemented and captured by steps 3–5 and 11 in the flow chart to update the proportion of surviving nodes.

In the third restorative resilience stage, compared with the original power grid, a resilience-improved system is assumed to have shorter recovery response time (reflected in step 6) and better recovery sequences (reflected in step 7 and propagated through steps 8–12). For the original power grid, the response time is 4 h and the recovery sequences are determined randomly. These assumptions are based on practical experience soon after disruption occurs. Typically, failures are reported by inefficient channels, such as calls by customers, leading to incomplete information and delays in failure detections by operators. This then leads to recovery sequences that are not optimized and are usually based on the time order of the failure reports. For the resilience-improved grid, the response time is only 1 h and the recovery sequences are selected according to the maximum node and link betweenness. The larger the component betweenness, the closer its topological distance (shortest path length) with the generators, and its priority restoration is heightened.

According to above assumptions, this paper considers five system cases to analyze and compare the effectiveness of the offered improvement strategies at different stages: Case 0 is the original grid, case 1 is the original grid with improvements in resilience stage 1, case 2 is the original grid with improvement in stage 2, case 3 is the original grid with improvements in resilience stage 3, and case 4 represents the original grid with improvements in all three resilience stages.

3.3. Simulation results

This subsection analyzes the expected annual resilience of the five system cases and compares the effectiveness of different strategies under scenario hazards, random hazards, hurricane hazards, and multiple hazards.

3.3.1. Performance response curve for scenario events

From the simulation results, given q^h, the average performance response curve can be plotted for each hazard type. When the recovery cost r is 30 as a typical scenario of limited recovery resources in practice, Fig. 4a shows simulation results under random hazards with $q^1 = 3$, corresponding to the number of initial randomly failed components, while Fig. 4b presents simulation results under hurricane hazards with $q^2 = 3$, corresponding to the hurricane category. Note that the time scales are different for the two hazard types due to the different restoration times: hour scale for random hazards and day scale for hurricane hazards.

Case 1 enhances the resistant capacity by reducing the frequency v^1 of random hazards and ensuring smaller component failure probabilities under hurricane hazards. Under random hazards, the performance response curve overlaps with the original grid (Case 0) because in this plot the performance curve is the average

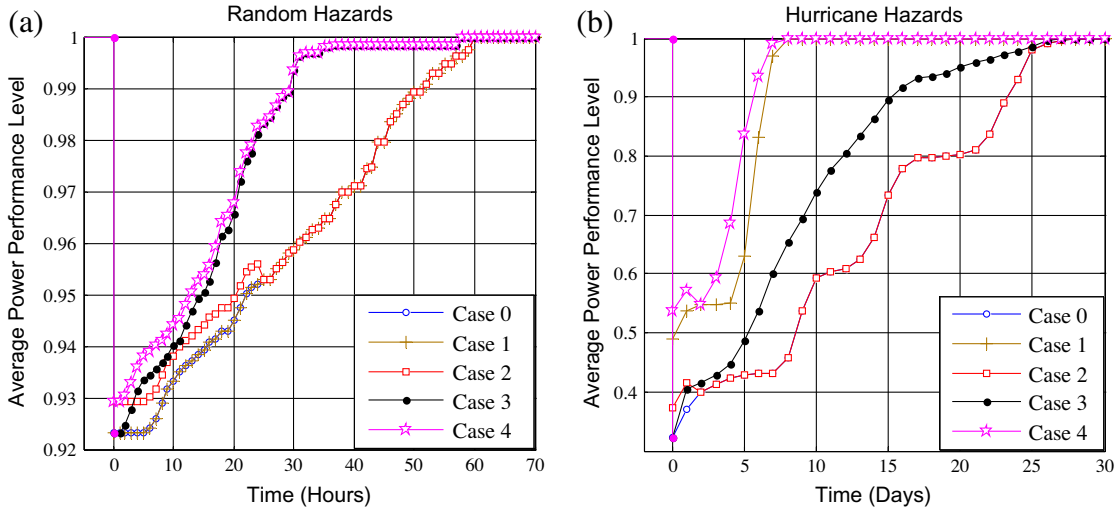

Fig. 4. Average performance response curves under singe hazards with a given scenario hazard intensity and $r = 30$ units of recovery resources. (a) Random hazards with intensity $q^1 = 3$, corresponding to the number of initial randomly failed components. (b) Hurricane hazards with intensity $q^2 = 3$, corresponding to the hurricane category.

system response under a given hazard intensity $q^1 = 3$ (scenario-based), which does not benefit from the reductions to the overall hazard frequency v^1. Under hurricane hazards, hardening some critical substations is very effective (even for a scenario event), not only for reducing the maximum impact level ($1 - I$ from 0.68 to 0.51) but also for enhancing the performance response curve due to less initial failed substations.

Case 2 improves the absorptive capacities to have energy storage units or emergency generators for critical substations. Its performance curve shows a decreased maximum impact level and enhanced curve during the redundant periods (first 24 h) under both hazard types. After depleting the redundant capacities, the system performance level decreases to be the same as that of the original grid. In addition, the effectiveness of redundancies under hurricane hazards is less obvious than under random hazards, because the redundant capacities (1 day) relative to the total restoration time under hurricane hazards (from days to weeks and even months) are much smaller than under random hazards (several hours to a few days).

Case 3 improves the restorative capacity to have rapid recovery responses and better recovery sequences. Under random hazards, the performance curve clearly shows the effects of prompt and properly sequenced responses, as components start being restored after 1 h relative to 4 h for the original grid. The effectiveness is clearly shown in both hazard types—especially under random hazards. The recovery speeds (slopes of the recovery part of the average performance response curves) increase and the impact area reduces considerably.

Finally, when all three-stage improvement strategies work together (Case 4), the impact areas under both hazard types are reduced by almost 50% relative to that of the original grid.

3.3.2. Resilience under single hazards

The simulation results also provide the expected impact areas $E[AIA^h(q^h)]$ given different q^h levels. Hence taking the hazard frequency and the distribution of the hazard intensities into consideration the calculation of the expected annual resilience is enabled for single hazards according to Eq. (12) with $H = 1$. Fig. 5 shows these results.

With an increase of r, the expected annual resilience increases for each case, and finally reaches a steady value. Deploying redundancies is the least effective strategy (Case 2), which is due to the small redundant capacities for this kind of infrastructure system (only 24 h). Adopting better recovery sequences (Case 3) is the most effective single strategy, particularly under limited recovery resources. When r is large, different single improvements are equally effective under hurricane hazards, while prompt responses work best for random hazards because of the smaller restoration times.

When all three-stage improvements work together, the expected annual resilience improves significantly. However, for the hurricane hazards, the improvement magnitude of Case 4 becomes negligible relative to the random hazards under sufficient r. This is mainly because the hurricane damaged components require long restoration times so that accelerating the response time (Case 3, a few hours ahead to start restoration) and deploying small-capacity redundancies (Case 2, one day) contribute little to resilience improvement.

In addition, although in Fig. 4b hardening critical components (Case 1) is the optimum strategy to reduce the impact area under hurricane category 3, in Fig. 5b adopting a better recovery sequence (Case 3) is the best strategy. This is because hurricanes with category 1 and 2 hardly cause substation damage and only lead to some line failures, so hardening substations takes no effect for such hurricanes, which account for 72% (Table 2) of all hurricane events. Hence, Case 3 has a larger expected annual resilience than Case 1 when considering hazard frequencies in the resilience metric.

3.3.3. Resilience under multiple hazards

This subsection analyzes the expected annual resilience under multiple hazards in terms of Eq. (12) with $H = 2$. Fig. 6 shows that the strategy of accelerating recovery responses and adopting better recovery sequences in stage 3 is still the optimum one, particularly under limited recovery resources r. Specifically, when r is only 10 units, the improvement magnitude (relative to Case 0) of the expected annual resilience of Case 3 is 25 times that of Case 2 and 4.4 times that for Case 1. Under sufficient r, the improvement magnitude becomes smaller and it is only 2.7 times that for Case 2 and 1.6 times that for Case 1.

To compare the resilience under single hazards and the resilience under multiple hazards, Table 3 presents the value of the expected annual resilience in different cases when r is large (1000 units). From the table, for each system case, the expected annual resilience under hurricane hazards is larger than the resilience under random hazards, which indicates that the power transmission

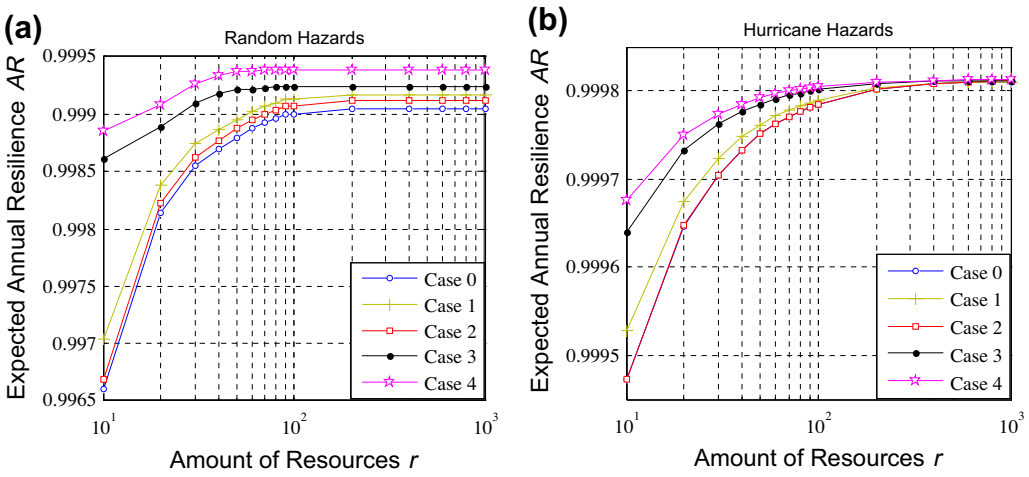

Fig. 5. Expected annual resilience *AR* under single hazards as a function of the amount of recovery resources *r* for different system cases. (a) Random hazards. (b) Hurricane hazards.

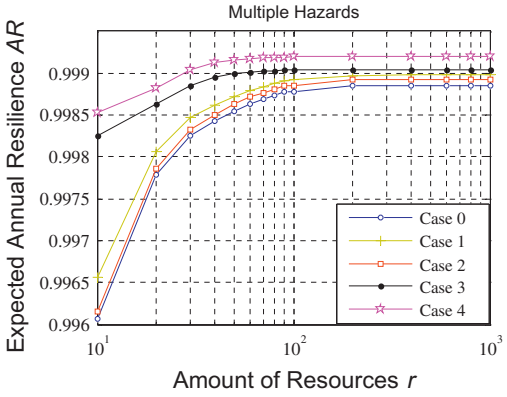

Fig. 6. Expected annual resilience *AR* under multiple hazards as a function of the amount of the recovery resources *r* for different system cases.

Table 3
Expected annual resilience for different system cases under single hazards and multiple hazards when the recovery resources are sufficient ($r = 1000$ units).

Hazard type	Case 0 (%)	Case 1 (%)	Case 2 (%)	Case 3 (%)	Case 4 (%)
Random hazards	99.9040	99.9170	99.9120	99.9240	99.9390
Hurricane hazards	99.9810	99.9810	99.9811	99.9812	99.9813
Both	99.8860	99.8980	99.8930	99.9050	99.9200

system in Harris County is more resilient under hurricane hazards. This is mainly due to the small annual hurricane frequency (1/7 while it is 19 for random hazards). Hence, to easily improve the expected annual system resilience, efforts can focus on protection from random hazards, although these efforts will not necessarily be sufficient to withstand rare events. Effective strategies to jointly address rare and typical events should be identified in a probabilistic optimization approach, where interaction effects of resource allocations are also explicitly modeled, thus going beyond the proposed *expected* annual resilience *AR*.

In addition, Table 3 shows that when the three-stage strategies work together, under different hazard types, the improvement magnitudes relative to the original grid are 0.035% for random hazards, 0.0003% for hurricane hazards and 0.034% under multiple hazards. To verify the robustness of these results, it is possible to compute the scenario-based resilience distribution from $AR' = \int_0^T P(t)dt / \int_0^T TP(t)dt$, whose expected value is tantamount to the resilience in Eq. (1). With the scenario-based resilience distribution from different hazard cases, and given a significance level of 0.05, the confidence intervals for the improvement magnitudes are respectively estimated as [0.026%, 0.044%] for random hazards, [0%, 0.002%] for hurricane hazards and [0.025%, 0.043%] under multiple hazards. These relatively small intervals indicate that the obtained resilience improvement results are robust, despite the resilience model having many input parameters and small absolute expected resilience values.

Although the obtained improvement levels are small in absolute terms, the saved economic losses may be significant. This is because if the performance level metric is the fraction of customers without outage instead of the proportion of surviving nodes, the expected annual resilience metric will equal to the power reliability metric used in the industry—the Average Service Availability Index (ASAI), which is the ratio of the total number of customer hours in which service was available during a given time period to the total customer hours demanded. The two performance level metrics are strongly correlated, so the expected annual resilience in this paper has similar features to the power reliability metric. The reliability of the US power grid (with transmission line-length of approximately 300,000 km) is 99.97%, and the 0.03% unreliability level costs the economy $150 billion per year [40]. The transmission line length in Harris County is 2 144.5 km; hence, according to the line length ratio from the county to national level (2144.5/300,000 = 0.007), a small resilience improvements may still save millions of dollars per year in Harris County, Texas.

4. Conclusions

The performance response process of an infrastructure system following a disruptive event is divided into three stages, reflecting system resistant, absorptive and restorative capacities. These capacities together determine system-level resilience in a quantitative fashion. Taking the power transmission grid in Harris County, Texas as an example, this paper uses a practical power grid model and several hypothetical resilience-improved models to compute their expected annual resilience under random hazards and hurricane hazards. Results show that the expected annual resilience is mainly compromised by random hazards due to their higher frequency relative to hurricane hazards. In addition, under limited recovery resources, adopting better recovery sequences is the overall optimum single strategy. Under sufficient recovery

resources, deploying redundancies, hardening critical components and rapid recovery responses tend to be similarly effective. In addition, the expected annual resilience of the power grid with all three-stage improvements increases 0.034% compared to the original grid when recovery resources are not severely constrained. The improvement is small, but it may save millions of dollars per year in aggregate in the context of real power grid reliability performance as assessed by energy experts.

Details of the proposed framework can be further refined in the future. First, other dimensions of resilience, such as social, organizational and economic, should be addressed to provide a comprehensive resilience analysis by using other parameters as the performance level metrics, such as the availability of critical facilities, the number of people served, or the level of economic activities. Second, this paper provides a general formulation for the expected annual resilience that is adequate for single hazards and multiple hazard types including inter-hazard interactions, but the example only addresses the case of inter-hazard independence for illustrative purposes. Further studies on the inter-hazard interactions due to preventive strategies are partially discussed in another study [41], but their formal treatment and the optimal inter-hazard interactions from co-occurrences of different hazard types are still the subjects of future studies. Third, this paper only considers a few resilience-based improvement strategies, while other strategies (expanding Table 1) together with their estimated cost can also be explored to find the optimum retrofit strategies for multiple hazards under limited budget as in life-cycle cost–benefit studies, allowing going beyond expected values of annual resilience. Fourth, it is also worth to incorporate the proposed resilience analysis into larger frameworks of infrastructure performance analysis, including their interdependencies [42], such as the resilience parameter in dynamic input–output inoperability models [43,44], along with their potential coupling with network-based methods and the achievement of target risk-based design provisions.

Acknowledgements

This material is based upon work supported in part by the National Science Foundation under Grants CMMI-0728040 and CMMI-0748231. Any opinions, findings, and conclusions or recommendations expressed in this material are those of the authors and do not necessarily reflect the views of the National Science Foundation. The authors also wish to thank Rice University and the Office of Public Safety and Homeland Security of the City of Houston for their support.

References

[1] Rinaldi SM, Peerenboom JP, Kelly TK. Identifying, understanding, and analyzing critical infrastructure interdependencies. IEEE Cont Syst Mag 2001:11–25.
[2] Shinozuka M, Dong X, Chen TC, Jin X. Seismic performance of electric transmission network under component failures. Earthq Eng Struct Dyn 2007;36:224–7.
[3] Dueñas-Osorio L, Vemuru SM. Cascading failures in complex infrastructure systems. Struct Safety 2009;31:157–67.
[4] Ouyang M, Dueñas-Osorio L. An efficient approach to compute generalized interdependent effects between infrastructure systems. J Comput Civil Eng. 2011. <http://www.dx.doi.org/10.1061/(ASCE)CP.1943-5487.0000103>.
[5] Rosato V, Issacharoff L, Tiriticco F, Meloni S. Modeling interdependent infrastructures using interacting dynamical models. Int J Crit Infrastruct (IJCI) 2008;4(1–2):63–79.
[6] Bruneau M, Chang SE, Eguchi RT, et al. A framework to quantitatively assess and enhance the seismic resilience of communities. Earthq Spectra 2006;19(4):737–8.
[7] Vugrin ED, Warren DE, Ehlen MA, Camphouse RC. A framework for assessing the resilience of infrastructure and economic systems. In: Kasthurirangan C, Gopalakrishnan, Srinivas Peeta, editors. Sustainable and resilient critical infrastructure systems: simulation, modeling, and intelligent engineering. Berlin: Springer-Verlag, Inc.; 2010.
[8] Reed DA, Kapur KC, Christie RD. Methodology for assessing the resilience of networked infrastructure. IEEE Syst J 2007;3(2):174–80.
[9] Cimellaro G, Reinhorn A, Bruneau M. Seismic resilience of a hospital system. Struct Infrastruct Eng 2010;6(1):127–44.
[10] Obama B. Presidential proclamation for national preparedness month. The White House (September 4, 2009). http://www.whitehouse.gov/the_press_office/Presidential- Proclamation-National-Preparedness-Month/ (accessed 28.09.09).
[11] Holling CS. Resilience and stability of ecological systems. Annu Rev Ecol Syst 1973;4:1–23.
[12] US Department of Homeland Security, National infrastructure protection plan, partnering to enhance protection and resiliency, 2009. <http://www.dhs.gov/xlibrary/assets/NIPP_Plan.pdf>.
[13] Haimes YY. On the definition of resilience in systems. Risk Anal 2009;29(4):498–501.
[14] Aven T. On some recent definitions and analysis frameworks for risk, vulnerability and resilience. Risk Anal 2011;31:515–22.
[15] Kahan JH, Allen AC, George JK. An operational framework for resilience. J Homeland Sec Emerg Manage 2009;6(1). article 83.
[16] Chang SE, Shinozuka M. Measuring improvements in the disaster resilience of communities. Earthq Spectra 2004;20(3):739–55.
[17] Bruneau M, Reinhorn AM. Exploring the concept of seismic resilience for acute care facilities. Earthq Spectra 2007;23(1):41–62.
[18] Cimellaro G, Reinhorn A, Bruneau M. Framework for analytical quantification of disaster resilience. Eng Struct 2010;32:3639–49.
[19] Zobel CW. Representing perceived tradeoffs in defining disaster resilience. Decision Support Syst 2010;50:394–403.
[20] Shinozuka M. Resilience of integrated power and water system, research progress and accomplishments, 2003–04. Buffalo (NY): MCEER.
[21] Leveson N. A new accident model for engineering safer systems. Safety Sci 2004;42(4):237–70.
[22] Straub D, Der kiureghian A. Bayesian network enhanced with structural reliability methods: methodology. J Eng Mech 2010;136(10):1248–58.
[23] Sakis-Meliopoulos AP, Cokkinides G, Huang R, Farantatos E, Choi S, Lee Y, et al. Smart grid technologies for autonomous operation and control. IEEE Trans Smart Grid 2011;2(1):1–10.
[24] Pepyne DL. Topology and cascading line outage in power grids. J Syst Sci Syst Eng 2007;16(2):202–21.
[25] Ouyang M, Yu MH, Huang XZ, Luan EJ. Emergency response to disaster-struck scale-free network with redundant systems. Physica A 2008;387(18):4683–91.
[26] Pahwa S, Hodges A, Scoglio C, Wood S. Topological analysis of the power grid and mitigation strategies against cascading failures. In: 2010 4th Annual IEEE systems conference, San Diego, CA. p. 272–6.
[27] Nezam-Sarmadi SA, Nouri-Zadeh S, Azizi S, Rahmat-Samii R, Ranjbar AM. A power system build-up restoration method based on wide area measurement systems. Eur Trans Electr Power 2011;21(1):712–20.
[28] Mota A, Mota LTM, Morelato A. Visualization of power system restoration plans using CPM/PERT graphs. IEEE Trans Power Syst 2007;22(3):1322–9.
[29] National Hurricane Center, 2010. <http://www.nhc.noaa.gov/pastprofile.shtml>.
[30] Wen YK, Kang YJ. Minimum building life-cycle cost design criteria. I: Methodology. J Struct Eng ASCE 2001;127(3):330–7.
[31] Wen YK. Structural load modeling and combination for performance and safety evaluation. New York: Elsevier Science; 1990.
[32] Platts, 2009. <http://www.platts.com/>.
[33] Carreras BA, Newman DE, Dobson I, Poole AB. Evidence for self-organized criticality in a time series of electric power system blackouts. IEEE Trans Circ Syst 2004;51(9):1733–40.
[34] Dobson I, Carreras BA. Number and propagation of line outages in cascading events in electric power transmission systems. In: 48th annual allerton conference on communication, control & computing, IL, USA, 2010.
[35] Ouyang M, Dueñas-Osorio L. An approach to design interface topologies across interdependent urban infrastructure systems. Reliab Eng Syst Safety 2011;96(11):1462–73.
[36] Federal Emergency Management Agency. Hazards US Multi-Hazard (HAZUS-MH) Assessment Tool v1.3; 2008. <http://www.fema.gov/plan/prevent/hazus/index.shtm>.
[37] Winkler J, Dueñas-Osorio L, Stein R, Subramanian D. Performance assessment of topologically diverse power systems subjected to hurricane events. Reliab Eng Syst Safety 2010;95(4):323–36.
[38] Anghel M, Werley KA, Motter AE. Stochastic model for power grid dynamics. In: 4th Hawaii international conference on system sciences, 2007, Big Island, Hawaii.
[39] Center for Energy and the Global Environment. <http://www.ceage.vt.edu/energy_storage>.
[40] National Institute of Standards and Technology. White paper: energy-technologies to enable a smart grid. <http://www.nist.gov/tip/wp/upload/energy_wp_10_28_10.pdf.2001>.
[41] Ouyang M, Dueñas-Osorio L. Time-dependent resilience assessment and improvement for urban infrastructure systems. Chaos, submitted for publication.
[42] Hernández I, Dueñas-Osorio L. Sequential propagation of seismic fragility across interdependent lifeline systems. Earthquake Spectra 2011;27(1):23–43.
[43] Haimes YY, Horowitz BM, Lambert JH, Santos JR, Lian C, Crowther KG. Inoperability input–output model for interdependent infrastructure sectors. I: Theory and methodology. J Infrastruct Syst 2005;11(2):67–79.
[44] Santos JR, Haimes YY. Modeling the demand reduction input–output (I–O) inoperability due to terrorism of interconnected infrastructures. Risk Anal 2004;24(6):1437–51.